MINISTRY OF EDUCATION
TECHNICAL UNIVERSITY
OF CLUJ-NAPOCA, ROMANIA

Electronics, Telecommunications and Information Technology

PhD THESIS
– ABSTRACT –

Research into accurate measurement of a wire position through optoelectronics methods

PhD Student:
Adrian Mocan

PhD Supervisor:
Prof. Eng. Ioan CIASCAI, PhD

Examination committee:
Chair: Prof. Eng. **Dorin Petreuş**, PhD – Technical University of Cluj-Napoca;
PhD Supervisor: Prof. Eng. **Ioan Ciascai**, PhD – Technical University of Cluj-Napoca;
Members:
- Prof. Eng. **Aurel-Ștefan Gontean**, PhD – Politehnica University of Timișoara;
- Prof. Eng. **Petre-Lucian Ogruțan**, PhD – Transilvania University of Brașov;
- Prof. Eng. **Dan Pitică**, PhD – Technical University of Cluj-Napoca.

– Cluj-Napoca –
2021

Contents

Context, Motivation and Objectives of Thesis

Monitoring the structural integrity of dams is a vital activity. Good monitoring of dams prevents their failure, which can cause great loss of property and lives.

In the current period, in the field of hydro-technical civil engineering, the emphasis has shifted from the construction of dams to their monitoring. This change of emphasis is because the existing hydropower potential has been almost entirely developed, as well as to the fact that the existing dams are starting to be over 50 years old, after which the need for monitoring becomes greater.

In order to facilitate a better monitoring of dams, this thesis aims to improve the methods of measuring relative displacement. Relative displacement is an important indicator for dam monitoring, which shows how certain components of a dam move relative to other components of the dam. Specifically, the relative displacement is measured using pendulum installations, where the position of the pendulum wire is measured in a horizontal plane.

As concrete objectives, the thesis aims to bring improvements in the reduction the cost of production of the measurement instrument for the wire position, as well as improvements to the accuracy of wire position measurement. For wire measurement accuracy, the goal is to obtain an accuracy better than 100µm, for both measuring axes.

The Structure of the Thesis

The thesis is structured in three main parts: INTRODUCTION, CURRENT STAGE OF KNOWLEDGE and PERSONAL CONTRIBUTION. The detailed structure of the thesis can be seen in the chapter "Integral Contents of the Thesis".

INTRODUCTION

The INTRODUCTION part describes the issue of monitoring the structural integrity of dams.

Dam monitoring is performed using a variety of devices, which measure the internal parameters of dams, as well as environmental factors. An important measure for monitoring the structural integrity of dams is relative displacement. It measures how some parts of the dam move relative to other parts. Pendulum systems are used to measure relative displacement.

A pendulum installation consists of a weight of a few kilograms, suspended by a steel wire with a diameter of about 1 mm and a length of several tens of meters. The weight is placed in a liquid tank that has the role of damping the oscillations of the pendulum. Typically, the steel wire is suspended from the top of the dam. Near the end where the weight is suspended, the displacement of the wire in a horizontal plane is measured with respect to the dam structure. This displacement indicates how much the upper part of the dam moves horizontally with respect to the lower part.

STATE OF THE ART

This part reviews the current state of scientific knowledge in the field of measuring the position of the pendulum wire to determine the relative displacement for dams (Chapter 1).

At the beginning, two types of errors (which can affect the measurement results) commonly encountered in the practice of measurements are described. A major source of errors is given by horizontal air currents flowing over the pendulum wire (Chapter 1.1). It is shown how an air stream with a speed of only 5km/h, circulating over a wire with a diameter of 1mm, over an exposed length of 2m (at the mobile end of the pendulum), from the total length of the wire of 50m, at the end of which hangs a 20kg weight, will deviate by 1mm. This deviation produced by realistic quantities is an order of magnitude larger than the measurement error imposed by the accuracy set in the objective. Another major source of error described has its effects after the commissioning of the pendulum system. This error is caused by the fact that the steel wire used in the pendulum installation is usually stored in the warehouses coiled (Chapter 1.2). When the wire is stretched to make the pendulum installation, it will not be perfectly straight, but will acquire a helical shape, due to its storage in the form of a coil. It is shown that a steel wire with a diameter of 1mm (with Young's modulus of $2 \cdot 1011$ Pa) kept in the form of a coil with a radius of 15cm longer, will produce a spiral with a radius of 0.3mm, i.e. errors 6 times greater than the measurement errors imposed by the accuracy set out in the research objective.

This type of error gradually disappears over a period of several months, during which the steel wire is stretched under the effect of the suspended weight. Although this error disappears, its effect is important, because this error occurs in the period when the pendulum system is put into operation, which is when reference measurements are usually made. To combat this error, the pendulum wire can be subjected to a stretching procedure prior to its use in the pendulum measuring system.

Measurements that are performed by a human operator have been used traditionally to measure relative displacement (Chapter 1.3). One of the devices is the coordiscope (Chapter 1.3.1), to which a human operator adjusts a micrometric screw for each axis, so that the wire is targeted with an optical instrument. Another type of instrument used is the coordimeter (chapter 1.3.2). This instrument uses two rods that touches the wire and directly display the position of the wire, without the operator adjusting anything. This device has the disadvantage that the rods used act with a certain force on the wire and thus errors can be introduced in the measurements, especially when the wire is very long, the suspended weight is lighter or if several coordimeters are used on the same wire.

A more recent evolution with the development of electronics is the automatic measurement (chapter 1.4) of the position of the wire and its remote transmission. By automatically reading the wire position, data can be collected more often at a lower cost. This allows the application of more performant data analysis.

For the automatic measurement of the position of the wire, several measurement principles are used, each with their specific advantages and disadvantages.

The automatic measurement by contact with the pendulum wire (chapter 1.4.1) uses the same principle as for the coordimeter, except that instead of reading the position of the rods directly, different kind position sensors are used.

Automatic inductive sensor measurement (Chapter 1.4.2) uses a paramagnetic material attached to the pendulum wire, which is placed into the magnetic field of two coils that surrounds it. The position of the wire is obtained from the difference between the inductances of the coils, which is determined by coupling the coils in turns, into an oscillating circuit and measuring its frequency. A variant of this principle determines only the equilibrium position between the two coils, when the same frequency is obtained. To measure the position, the coil assembly is moved until the equilibrium position is obtained. This measuring principle applies to each axis separately.

The automatic measurement by capacitive sensor (chapter 1.4.3) uses a metal cylinder attached to the wire, which acts as a plate in two capacitors formed with another two plates that surrounds the cylinder. The determination of the position is done by finding the difference between the capacitances of the two capacitors thus formed. There are several ways by which the capacitances of the two capacitors can be measured.

Automatic measurement by optical sensor (chapter 1.4.4) can be done by several methods: "Measurement by laser distance reading", "Measurement by opto-mechanical system", "Measurement by analysis of shadow produced by a single light source" and "Measurement by analysis of shadows produced by multiple light sources".

Laser distance measurement (Chapter 1.4.4.1) uses a cylinder attached to the pendulum wire and two or three laser distance reading systems, which measure the distance to the cylinder. After the corrections for the cylinder geometry, the position of the wire can be determined.

The measurement by opto-mechanical system (chapter 1.4.4.2) essentially makes an automation of the coordiscope, where an optical barrier replaces the targeting operation, and a microcontroller does the adjustment operation of the micrometric screw automatically.

The measurement by analyzing the shadow from a single light source (chapter 1.4.4.3) is done by determining the wire shadow on a linear optical sensor. This method has to be applied to each measuring axis.

The measurement by analyzing the shadow from multiple light sources (chapter 1.4.4.4) is also done by determining the shadow of the wire on a linear sensor, but in this case several light sources are used in turn, so that by analyzing the position of at least two shadows the position of the wire can be determined. This measuring principle uses a single optical system for both measuring axes.

PERSONAL CONTRIBUTIONS

This part describes the research carried out during the doctoral program, in order to achieve the objectives of the thesis. Before describing the research, the objectives of the research are set out (Chapter 2), as well as the general methodology of the research (Chapter 3). Next, is described in four chapters (4, 5, 6 and 7) the research carried out to achieve the following goals: “Study of measurement errors”, “Compensation of measurement errors”, “Simulation of measurement errors” and “Practical implementation followed by experimental measurements”. Each research is structured in six subchapters: Introduction, Objective/Working Hypothesis, Material and Method, Results, Discussions and optionally Conclusions.

Objectives

This chapter (Chapter 2) sets out the objectives of the research, namely to improve the performance of measuring devices for the relative displacement of dams. In particular, it is targeted at an instrument production cost as low as possible with which to ensure a measurement accuracy better than 100μm, on both measuring axes.

General methodology

As a general methodology (chapter 3) the measurement principle chosen for the measuring instrument is the measurement by analyzing the shadows from multiple light sources. This choice was made primarily due to the fact that this principle uses a single optical assembly to measure the position of the wire, on both measuring axes, thus resulting in a lower production cost.

Some thesis specific terms are defined here, in order to facilitate a clear understanding of the expression. Thus, the term "reading" defines the process of reading the position of the shadow of the wire, projected by an LED on the linear optical sensor. The measurement principle is briefly described in this chapter and can be seen in Figure 1.

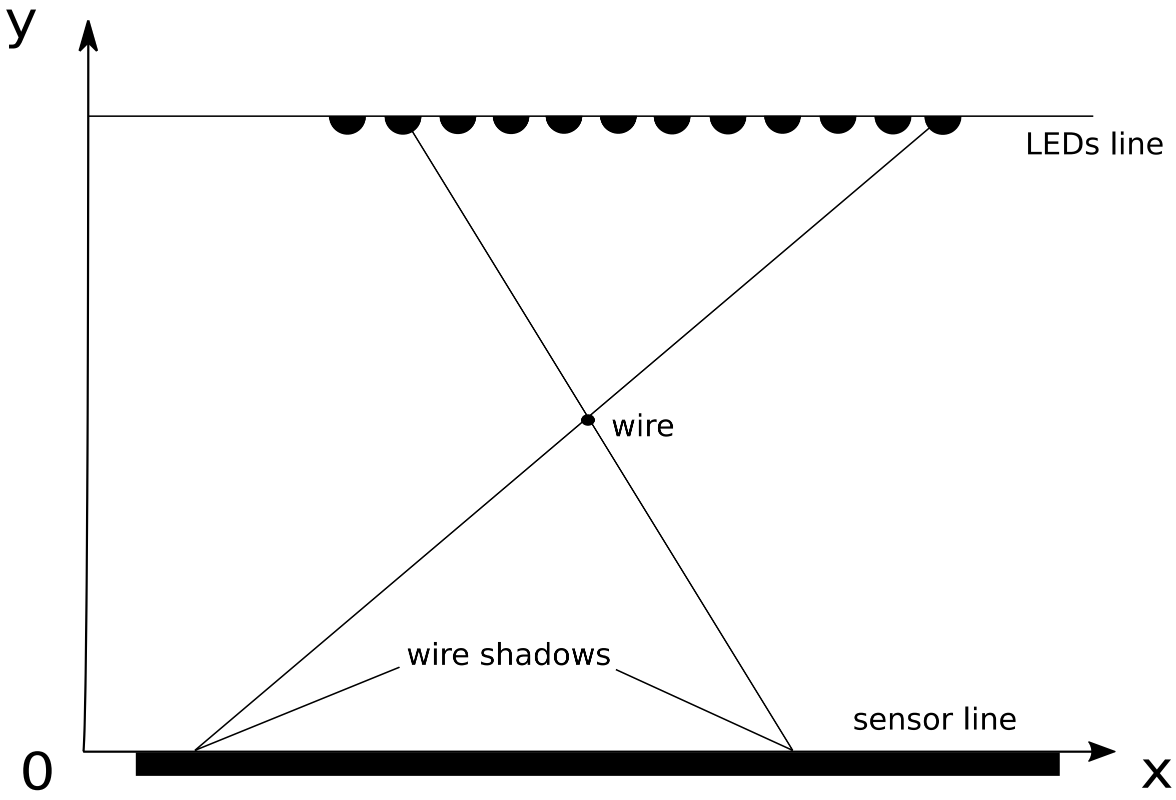

Figure 1: Measurement principle for the instrument

It can be seen in Figure 1 that the position of the wire is determined by the intersection of two lines, each given by the position of an LED and the shadow projected by it on the optical sensor.

Study of measurement errors

In this research (Chapter 4) are investigated the measurement errors of a measuring instrument, which implements the principle of analysis of shadows from multiple light sources, where only errors inherent of the operating principle are considered as sources of errors. In this way, the theoretical measurement limits of this type of instrument are investigated.

It is hypothesized that using an additional reading, with an LED chosen so that it will project a shadow, as perpendicular as possible onto the optical sensor, will improve the measurement accuracy for the X-axis.

The position of the wire is determined by writing similarity relations for the triangles formed by the rays of light that project the shadows. The measurement errors were determined by calculating the partial derivatives in relation to the quantities that affect the measurement. To simplify the calculations, a dimensionless quantity, *r*, has been introduced, which is determined by the distance between LEDs and the distance between shadows. Thus, the error of *r* is determined by both the positioning errors of the LEDs and by the errors in reading the position of the shadows. The position on the Y-axis depends directly on the *r*, so the error of the position on the Y-axis depends essentially on the error of *r*. For the X-axis, some other quantities were considered in the calculation of the errors were in addition to *r*. They are the position of the LED and the shadow from the third reading, as well as the origin alignment error for measuring the position on the X-axis for LEDs and shadows. This alignment error does not affect the position for the Y-axis, because the expression of the position on the Y-axis only includes the difference between the positions of the LEDs and between the positions of the shadows.

From the evaluation of the expression of the errors of r (which is a factor for both X-axis and Y-axis errors), it is found that in order to minimize them, it is necessary that the distance between the LEDs and between the shadows to be as great as possible. This gives the algorithm for finding the two LEDs with which the first two readings are made, for a given position of the wire: It starts with the LEDs at the margin and advances towards the center until a shadow is obtained on the optical sensor for each LED.

For the X-axis, the errors are analyzed to see how they are influenced by the third reading. It is found by evaluating the expression of errors, that using the third reading, the influence of r's errors decreases greatly in the expression of X-axis position. This will confirm the hypothesis according to which an additional reading reduces the errors on the X-axis. Confirmation of this hypothesis generates a method to improve X-axis accuracy, which is valuable in the context of this research, as it reduces X-axis position measurement errors without additional costs to the production of the measuring instrument.

Having the expression of the position errors for both measuring axes, a numerical evaluation of the errors for different wire positions in the measuring range is made, using the LED finding algorithm that ensures the minimum error for the wire position. To find a value for the LED positioning error, experimental measurements were performed on a usual LED strip.

The measurement errors for each wire position are expressed graphically according to the wire position, using a color scale to mark the magnitude of the errors. The error analysis shows that the dominant factor is the positioning error of the LEDs. In order to see the effects of a more accurate positioning of the LEDs, the error of positioning for LEDs was reduced to the level of the position errors of the shadows. After graphically expressing the errors in this case, it can be seen a reduction of the position measurement errors both as a value and as a distribution in the measuring range. This reduction confirms that indeed the positioning error of the LEDs is the dominant factor in measuring the position.

The conclusion of the study on measurement errors is that even just the errors inherent in the measurement principle (LED positioning errors and shadow position reading errors) are large enough to ultimately cause wire position measurement errors that exceed the target research(at least for certain areas of measurement domain). The largest measurement errors are on the Y-axis.

Error compensation

In this research (Chapter 5), we look for techniques to minimize the positioning error of LEDs, because these errors are dominant, as concluded in the study of measurement errors.

By calculating the positioning errors for the THT mounting technology, it was found that with this LED mounting technology on the PCB, the positioning errors will be too large for the need of LEDs precise positioning. These large errors are due to the diameter errors of the LED leads, as well as the fact that the technology requires an extra space between the leads and the edges of the holes.

For the SMT mounting technology there are too many unknown factors to be able to calculate the positioning accuracy of the LEDs on the PCB. For this reason, data on the positioning accuracy provided by the manufacturers of first assembly were sought. The positioning accuracy of the components offered by several manufacturers is good enough for the requirements of the instrument, so we tried to use several types of LED strips. Practical measurements show that the positioning error for the LEDs in SMD technology is 12 times higher than that offered by manufacturers. An explanation for this difference in error is due to the fact that manufacturers do not specify for which type of components they offer this accuracy. It is assumed that this high accuracy provided by manufacturers refers to integrated circuits that are positioned with fiducial marks. Finally, it was concluded with the practical measurements, that the SMT mounting technology does not ensure a sufficient positioning accuracy of the LEDs in this case (precise positioning of the LEDs for the measuring instrument).

Because the existing technologies for mounting the LEDs on the PCB do not ensure sufficient positioning accuracy, another way was sought in order to increase the positioning accuracy of the LEDs. Further research to increase the positioning accuracy of LEDs is based on the fact that the installation for instrument testing is able to position a simulated wire inside the measuring range with an accuracy of 5μm. Using the wire position as a reference and the position of the shadow/shadows projected by an LED, the position of the LEDs can be determined with better accuracy than their positioning accuracy on a PCB. These computationally determined LED positions, which provide superior accuracy, are to be stored in non-volatile memory and used in wire positioning calculations.

To find the position of the LEDs by calculation, depending on the position of the simulated wire and shadows, three methods have been developed that offer different advantages, depending on the complexity of each.

The single-read calibration method (Chapter 5.3.1) is the simplest method and determines for the LED only the position on the X-axis. The position of the shadow together with the position of the simulated wire determines the line representing the light beam. By intersecting this line with the line that represents the row of LEDs, the position of the LED on the X-axis is obtained.

The two-reading calibration method (Chapter 5.3.2) uses the shadows from the simulated wire, positioned in two different positions. The two different positions, together with the corresponding shadows, determine two lines that represent the light beams. The point of intersection of the two lines will determine the position of the LED, both on the X-axis and on the Y-axis.

The four-reading calibration method (chapter 5.3.3) comes to solve a practical problem. In practice, for one- and two-reading methods, the coordinate system of the measuring instrument must be aligned with the coordinate system of the test installation, with sufficient accuracy not to affect the positioning accuracy of the LEDs being calculated. The four-reading calibration method uses the positioning of the simulated wire in four positions that form the corners of a rectangle. This configuration allows the position of an LED to be calculated on both the X- and Y-axes, without the need to add or subtract positions in different coordinate systems. Therefore, this method allows the elimination a precise alignment between the origins of the two coordinate systems.

During the development of these methods, the presence of another source of errors was found in the measurement instrument. This source of errors has been identified as the refraction of the light beam at the interface between the air and the LED case and at the interface between air and the case of the optical sensor. To compensate for the refraction errors (Chapter 5.3.4) it was calculated how large the deviation of the light beam from the ideal position is, both for the position of the LEDs and for the position of the shadows. Having these deviations computed it is possible to compensate the errors introduced by the refraction of the light beam, by subtracting the deviation calculated from the position of the shadow and from the position of the LED.

The computed refraction errors were expressed as errors in positioning the LEDs and the shadows and they were plotted, depending on the angle of incidence. It can be seen from the graph that for an angle of incidence of 40 degrees, the error for measuring the position of the shadows reaches values of 250µm. A conclusion from the study of errors in Chapter 4 was that in order to obtain small measurement errors, the distances between LEDs and between shadows must be as great as possible which implies large angles of incidence. Unfortunately, these large angles of incidence will produce large refraction errors, hence the need to use error compensation for refraction errors.

The global calibration method (Chapter 5.3.5) was developed to compensate for LED positioning errors, refraction errors, and other types of errors, all with a single operation. The central idea is to use the test installation to make readings with all the LEDs for reference points positioned in a grid, which is spread throughout the measuring range. This collected data is to be stored in a non-volatile memory so that it can be used to correct errors that occur in measurements.

The simplest approach to this problem was to calculate the difference between the value of the purely geometrically measured position and the reference position for each point in the grid. For any other position, this difference can be interpolated to that position and the value of this difference can be used to correct the calculated position. It was found that in the case of this instrument, the grid interpolation method could be affected by the fact that different LEDs are used for different points, so that in the function to be interpolated will be discontinuities that affect the interpolation results.

In order to be able to correct measurement errors without the influence of switching from one LED to another, a new algorithm for correcting measurement errors has been developed that is using global calibration data. In essence, the algorithm tries to identify the reference points that surrounds the measurement point and to use the positions of the reference points shadows projected by the same LED. The algorithm uses a local interpolation of readings, with the positions of the reference shadows produced from the same LED, so that the problem of discontinuities introduced when switching from one LED to another is eliminated. In the limit case where four reference points with valid measurements from the same LED could not be identified, the algorithm uses for the position a value calculated based on the readings of a single reference point and the current readings. Because the error correction method based on global calibration addresses several types of errors, this error correction method was chosen to be used in the implementation of the measuring instrument.

Error simulation

In this research (Chapter 6), were studied using simulation, the values and the distribution of the measurement errors, produced by the most important error sources, as well as the error correction performance of the global calibration correction method. The sources of errors considered were the following: LED positioning, refraction produced at the LED case, refraction produced at the optical sensor case and quantization errors for reading the optical sensor.

The simulation principle starts from a given position of the wire, considered the true position. For this position the LEDs used are determined and then geometrically the corresponding shadows. To the values determined for the LED positions and to the shadow positions the errors that can occur are added. The measured position of the wire is obtained by intersecting the lines determined by the position of the LEDs with their corresponding shadows, when these positions are affected by the added errors. The difference between the determined position of the wire and the true position of the wire is considered to be the measurement error produced by simulation.

Because the simulation is using a whole algorithm for simulating error correction, not just a simple formula, a dedicated program was created for the simulation. To visualize the results, a program was created that graphically presents the measurement errors using a chromatic representation for the magnitude of the errors, depending on the position of the wire in the measuring range.

Using a graphical representation system similar to the graphical representation of the errors in Chapter 4, a visual comparison of the measurement errors obtained by the two different methods (calculation using partial derivatives and numerical simulation) is possible. This comparison is made for the case when only positioning errors of LEDs and quantization errors when reading the optical sensor are considered. The visual comparison of the two error calculation methods reveals a correlation between the error distributions, validating the correctness of the research results.

The representation of the cumulative errors from all error sources, which can be seen in Figure 2 and Figure 3, reveals that at least for the Y-axis the magnitude of the errors is too large to be able to make measurements with an accuracy of 100μm, without using an error correction method. In the figures showing the magnitude of the errors in the measuring range, the value of the errors is indicated chromatically. In dark blue are represented errors of 30μm or less and in red those of 200μm or greater. Errors with values between these two limits are represented using a color with a proportionally corresponding wavelength.

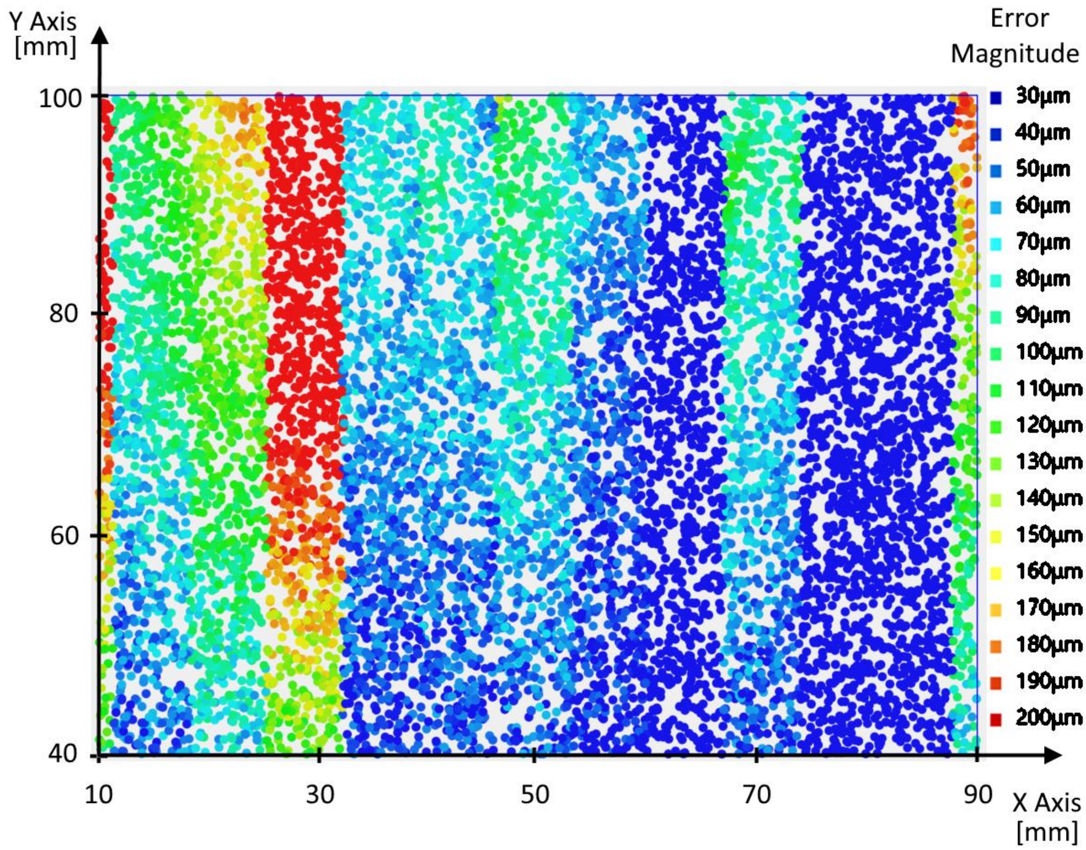

Figure 2: Distribution of errors from all sources combined, for X-axis

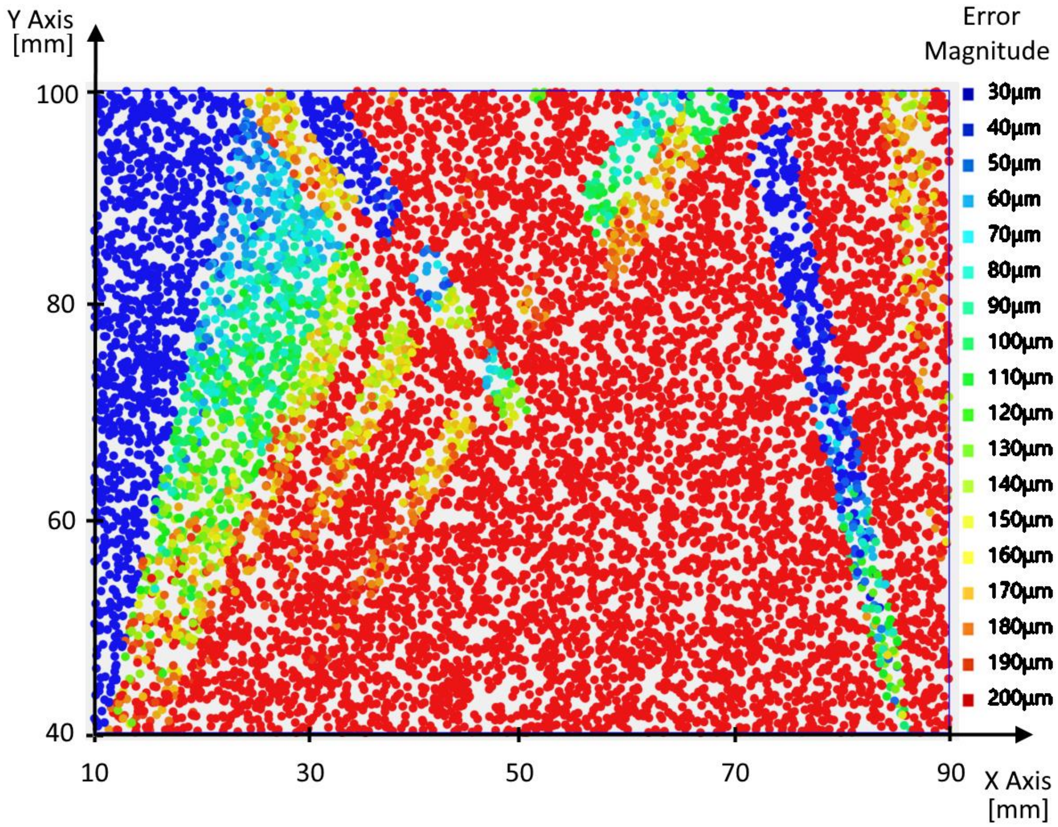

Figure 3: Distribution of errors from all sources combined, for Y-axis

After applying the "global calibration error correction method" to the measurement errors with all cumulative error sources, a significant error reduction was found. The error reduction is so good that allows a measurement with an accuracy better than 100µm, as specified in the research objective. The graphical representation of the measurement errors obtained after the error correction algorithm was applied can be observed in Figure 4 and Figure 5.

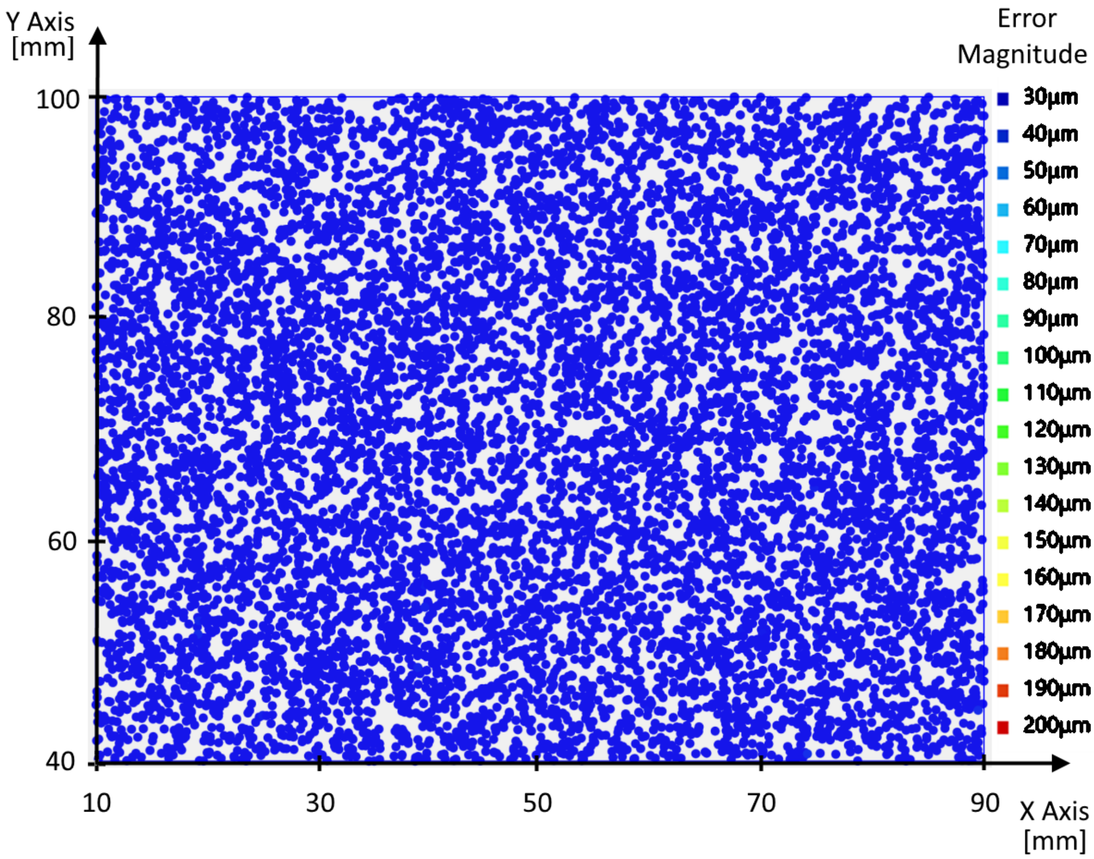

Figure 4: Distribution of errors after their correction, for X-axis

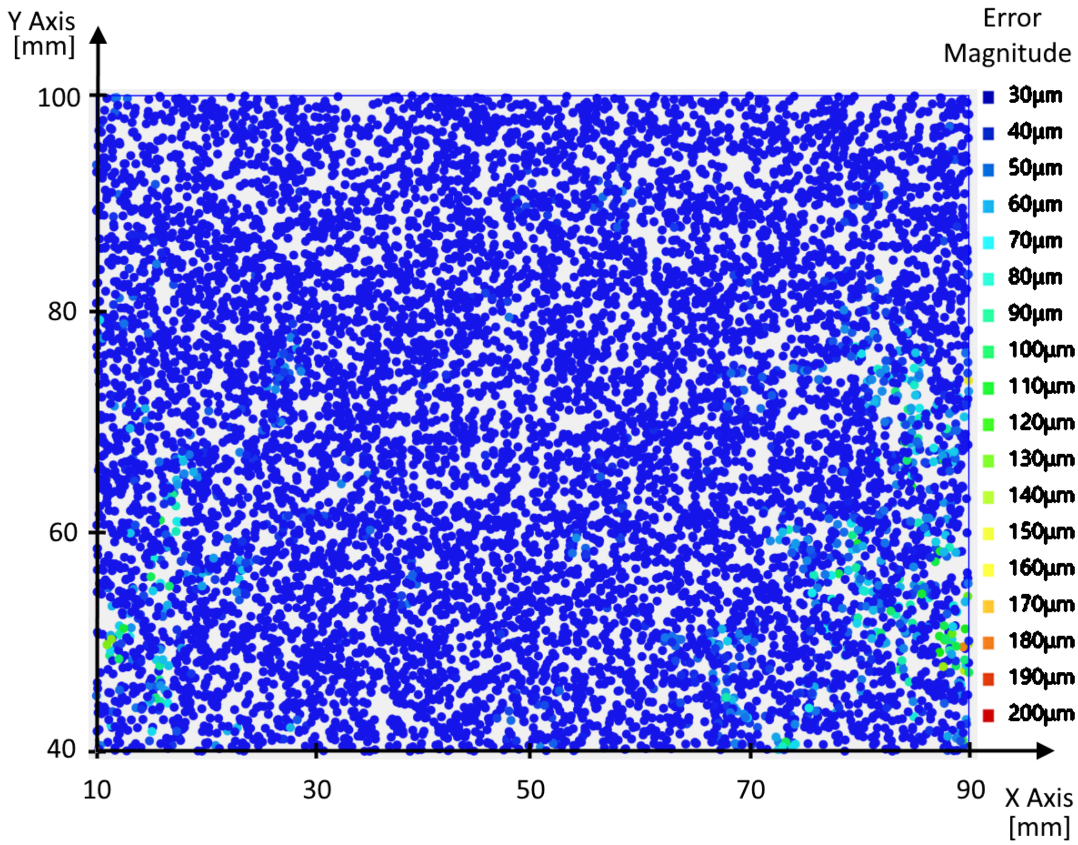

Figure 5: Distribution of errors after their correction, for Y-axis

Practical implementation and measurements

In this research (Chapter 7), methods were found to implement an experimental model for the measuring instrument. With the help of this experimental model, measurements were performed, in order to evaluate the measurement accuracy of the experimental model. Figure 6 shows the practical implementation of the experimental model.

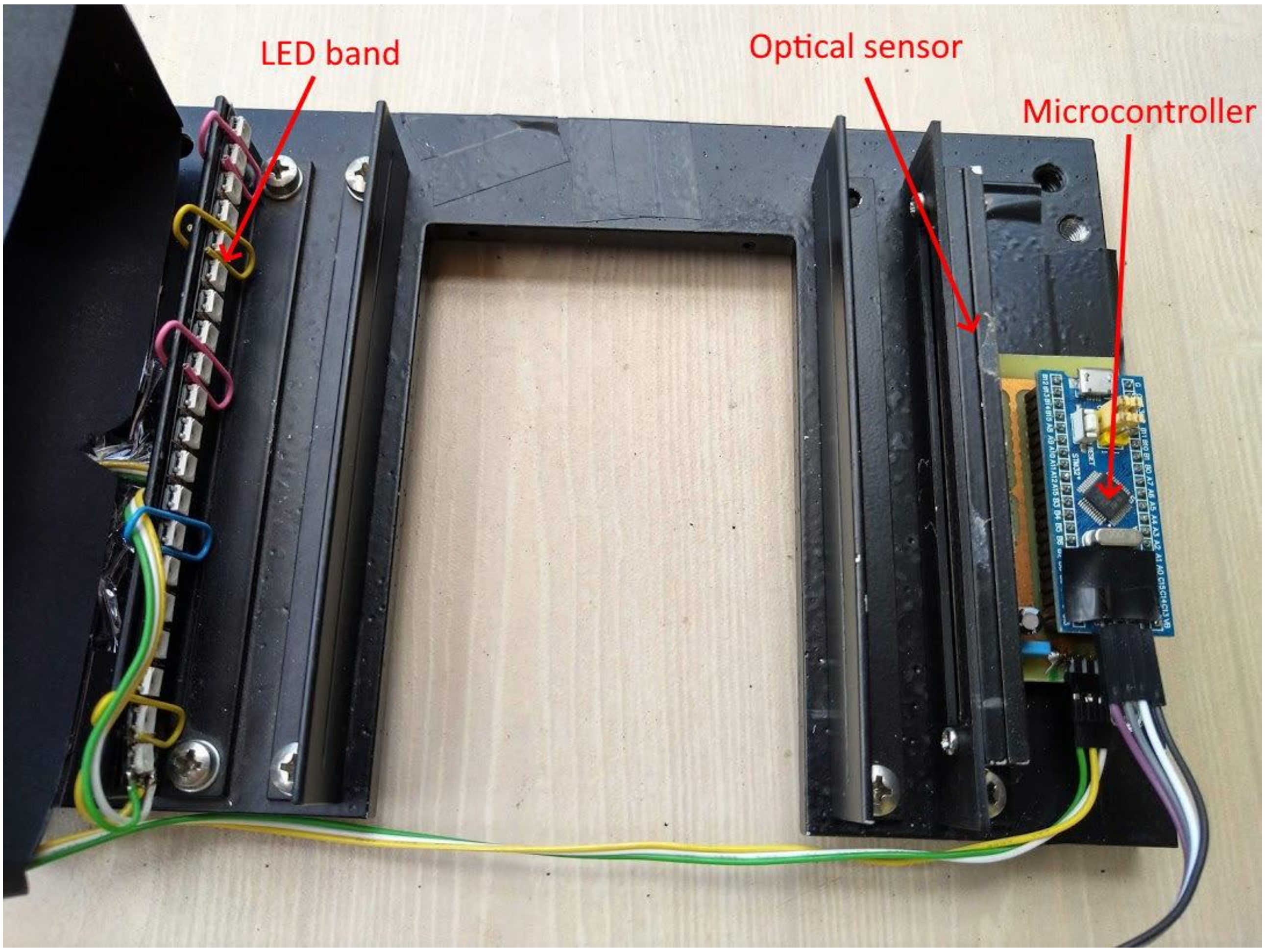

Figure 6: Picture of the experimental model

Chapter 7.3.1 describes the components chosen for the implementation of the electronic part of the measuring instrument, as well as the reasons that determined their choice. The chosen microcontroller is of the type STM32F103C8 , the chosen optical sensor is of the type TSL1412S, and the LED strip contains LEDs of type WS2812B.

The microcontroller program (chapter 7.3.2) coordinates the activity of measuring the position of the wire. For the control of the LEDs, the SPI interface was used together with a lookup table containing precomputed data, in order to achieve a more efficient control. An ADC converter with DMA for data transmission was used to read the optical sensor. A state machine has been implemented in order to control all the phases required for reading the optical sensor. The state machine generates the control signal for the ADC, thus accomplishing the sequence required to read the optical sensor.

Data taken from the optical sensor is used to determine the position of the shadow on the optical sensor. For this, a median filter is applied first to clean the noise of the optical signal. Then, a dynamic threshold is computed for the determination of the dark area, by taking a fraction from the result of another median filter, with a larger window. The dynamic threshold is required for the cases where an LED located at the margin of the LED strip is used. In this case, the brightness on the optical sensor is more pronounced on the LED side and decreases on the other side. The position of the shadow was considered in the middle of the area where the optical signal falls below the threshold of darkness.

The Measurements chapter (chapter 7.3.3) describes the test installation used for calibration, as well as the program that automatically performs the calibration of the instrument. The test installation is built like a numerical control machine, which can position a simulated wire with a precision of 5µm in the horizontal plane. This positioning is done by controlling the stepper motors, using the micro-stepping control mode.

Following the calibration of the device, a "virtual" coordinate system (generated by the calibration data) is obtained, so the instrument measurements are relative to this coordinate system.

After the calibration of the experimental model, the calibration data were stored and then used to correct measurement errors, using the global calibration correction method.

To evaluate the measurement performance of the experimental model, measurements of the wire position were performed, for several random positions of the simulated wire. Using statistical analysis on 175 measurements points, the following results were obtained:

- The standard deviation for absolute errors on the X-axis is 42µm
- The standard deviation for absolute errors on the Y-axis is 77µm

Following these results, the measurement accuracy of the experimental model can be declared with a confidence of 68%, as being ± 40µm on the X-axis and ± 80µm on the Y-axis.

A graphical representation of the measurement errors obtained in the experimental measurements with the experimental model is presented in Figure 7 and Figure 8.

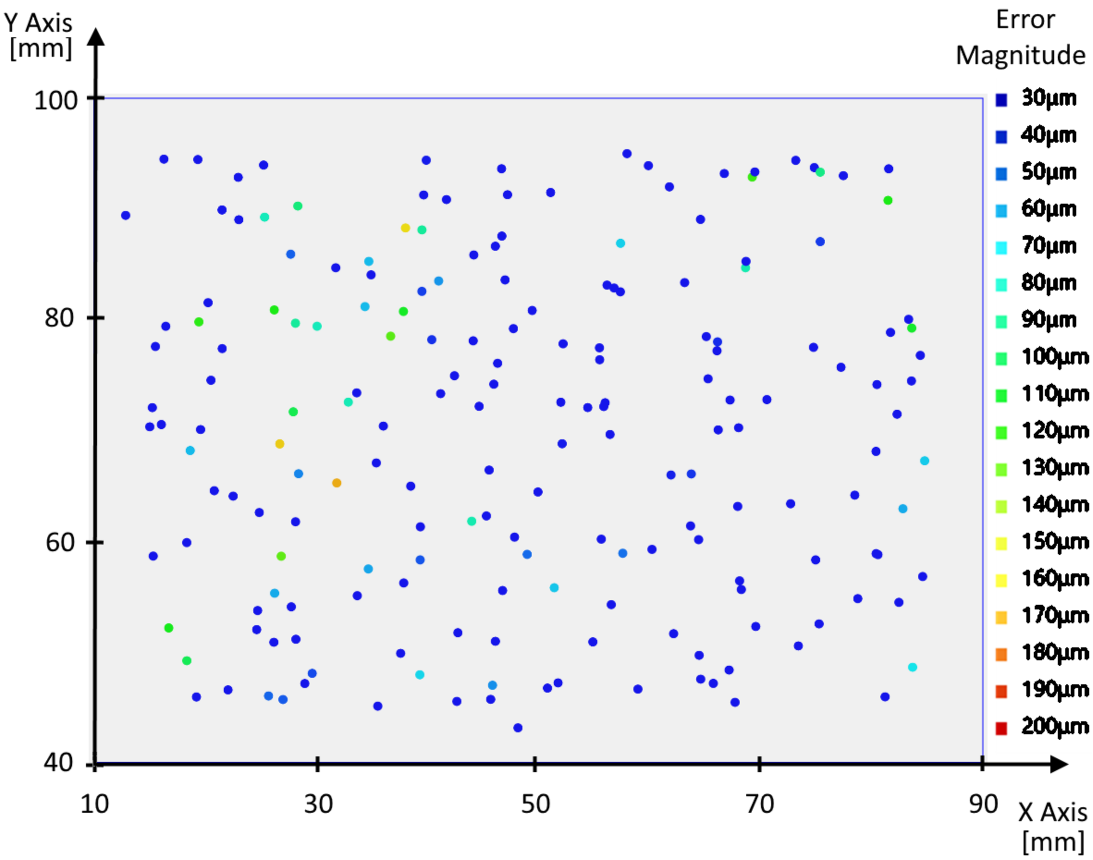

Figure 7: Measurement errors for X-axis

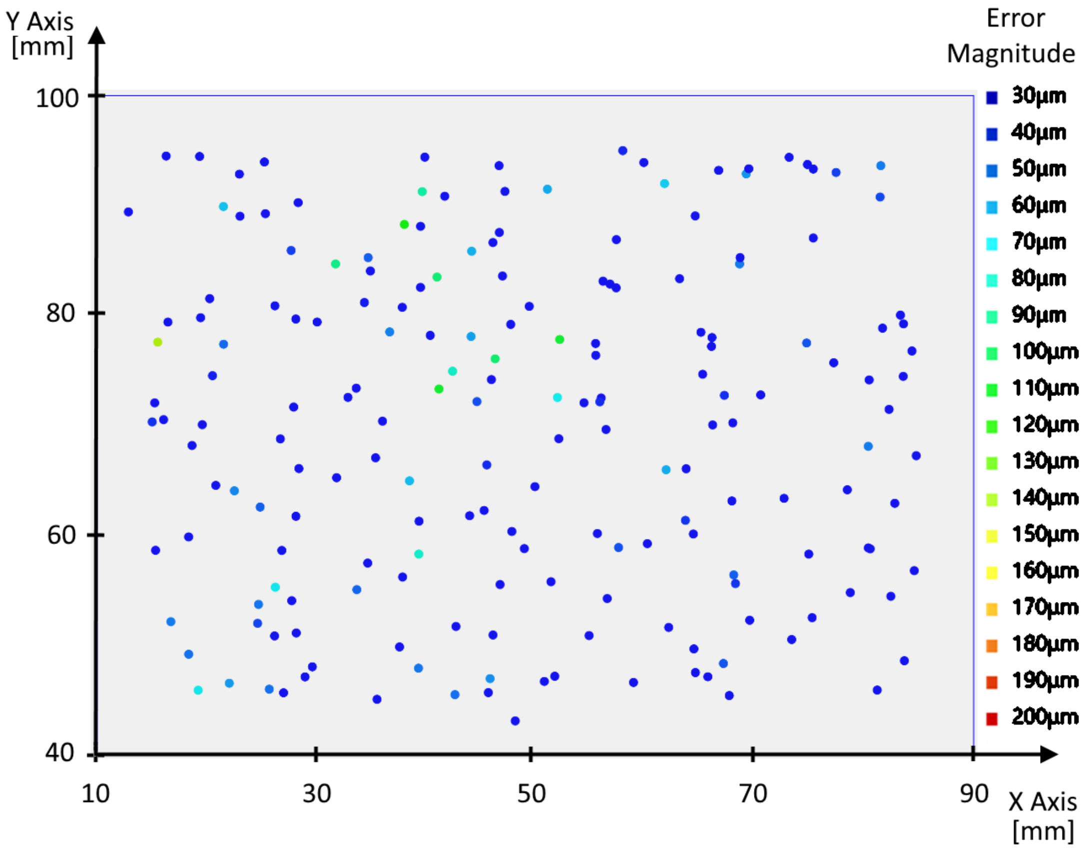

Figure 8: Measurement errors for Y-axis

General discussions

In this part of the thesis are presented considerations related to the results obtained and how they can be improved.

Another aspect considered (Chapter 8.1) is the procedure for installing the measurement instrument in the dam. In order to be able to guarantee the accuracy of the measurements, certain alignments requirements must be observed when installing the instrument in the dam. In order to be able to perform measurements in parallel with another existing instrument, it is necessary to execute a calibration procedure when installation in the dam is performed.

At the end of this part, future possible research directions are reviewed (chapter 8.2).

Final conclusions

This part presents the validation of research and the achievement of thesis objectives. It is considered that the set accuracy target has been reached by the measurement errors obtained (40µm for the X-axis and 80µm for the Y-axis), which are less than 100µm. The objective of reducing production costs is considered to be achieved by estimating a production cost four times lower than the cost for existing instruments on the market.

ORIGINAL CONTRIBUTIONS OF THE THESIS

The most important innovative elements developed in the thesis research are the following:

• Computing the value of inherent errors that occurs in a measurement instrument, which employs the principle of analyzing shadows from multiple light sources.

• Finding a way to improve the accuracy of the measuring instrument on the X-axis by introducing an additional reading.

• Finding ways to increase the accuracy of the instrument by calibrating the position of the LEDs.

• Finding a method to eliminate refraction errors that occur when light passes from the LED case into the air and then from the air into the optical sensor case.

• Finding a method to perform a global calibration of the instrument, so that there are no discontinuities due to switching from one LED to another.

• Simulation of several types of measurement errors that occur in an instrument which employs the principle of analyzing shadows from multiple light sources

• Simulation of measurement errors reduction obtained by when using error compensation with global calibration.

• Implementation of an experimental model of a measurement instrument that works on the principle of analyzing shadows from multiple light sources. The experimental model implements an error correction procedure, based on the global calibration method.

• Create a program that automatically guides the positioning of the wire and performs the readings required for the calibration procedure.

• Performing measurements with the experimental model and determining the accuracy of the experimental model using statistical analysis on the measurement results.

List of Publications

- [1] A. Mocan and I. Ciascai, “A model for measuring the position of a pendulum using opto-electronic method,” *Acta Tech. Napocensis - Ser. Appl. Math. Mech. Eng.*, vol. 61, no. 4, pp. 603–608, Dec. 2018. Indexat Web of Science: 000453442200011.

- [2] A. Mocan and I. Ciascai, “Analysis of positioning errors for LED,” in *2019 IEEE 25th International Symposium for Design and Technology in Electronic Packaging (SIITME)*, 2019, pp. 127–130. https://doi.org/10.1109/SIITME47687.2019.8990720, Indexat IEEE Xplore și Web of Science: 000564733700026.

- [3] I. Ciascai and A. Mocan, “Calibration procedure for pendulum position measurement,” *ACTA Tech. NAPOCENSIS - Ser. Appl. Math. Mech. Eng.*, vol. 63, no. 1, pp. 21–26, 2020. Indexat Web of Science: 000528235300003.

- [4] I. Ciascai and A. Mocan, “A practical implementation for an instrument to measure displacement of pendulum wire,” in *2020 International Symposium on Electronics and Telecommunications (ISETC)*, 2020, pp. 1–4. https://doi.org/10.1109/ISETC50328.2020.9301046, Indexat IEEE Xplore și Web of Science: 000612681000030.

- [5] A. Mocan, I. Ciascai, and A. Ciascai, “Simulations of Measurement Errors for a Pendulum Reader,” in *44th International Spring Seminar on Electronics Technology (ISSE)*, 2021, https://doi.org/10.1109/ISSE51996.2021.9467634, Indexat în IEEE Xplore.

The Full Contents of the Thesis

References

[1] E. Duflo and R. Pande, "Dams," *Q. J. Econ.*, vol. 122, no. 2, pp. 601–646, May 2007, doi: 10.1162/qjec.122.2.601.

[2] I.-A. Moldovan *et al.*, "The Rating of Large Romanian Dams into Seismic Risk Classes," *Resilient Soc.*, p. 121, 2017.

[3] W. Ge *et al.*, "A method for fast evaluation of potential consequences of dam breach," *Water (Switzerland)*, vol. 11, no. 11, p. 2224, Nov. 2019, doi: 10.3390/w11112224.

[4] C. A. Brown and W. J. Graham, "Assessing the threat to life from dam failure," *JAWRA J. Am. Water Resour. Assoc.*, vol. 24, no. 6, pp. 1303–1309, Dec. 1988, doi: 10.1111/j.1752-1688.1988.tb03051.x.

[5] *Safety of Existing Dams: Evaluation and Improvement - National Research Council, Division on Engineering and Physical Sciences, Commission on Engineering and Technical Systems, Water Science and Technology Board, Committee on the Safety of Existing Dams -*. National Academy Press, 1983. ISBN: 0-309-03387-X

[6] A. Popovici, R. Sarghiuta, I. Toma, and T. Moldoveanu, "Reevaluation of the seismic safety of a large arch dam commissioned thirty years ago," 1996, Accessed: Jun. 16, 2021. [Online]. Available: http://www.iitk.ac.in/nicee/wcee/article/11_1706.PDF

[7] C. Cragg, P. Hassan, and P. Toth, "A structured approach to assessing dam instrumentation and performance monitoring requirements," in *The Canadian Dam Association conference 2010: partnering for a safer future, Niagara Falls, ON (Canada*, 2010, pp. 1–13.

[8] P. Bukenya, P. Moyo, H. Beushausen, and C. Oosthuizen, "Health monitoring of concrete dams: a literature review," *J. Civ. Struct. Heal. Monit.*, vol. 4, no. 4, pp. 235–244, Oct. 2014, doi: 10.1007/s13349-014-0079-2.

[9] M. Wieland and B. H. Fan, "The activities of the International Commission on Large Dams (ICOLD) in the earthquake safety of large dams," Aug. 2004. Accessed: Jun. 16, 2021. [Online]. Available: https://www.researchgate.net/publication/268374291

[10] A. Popovici, "Ghid privind echiparea construcţiilor hidrotehnice de retenţie cu aparatură de măsură şi control," București, 2010.

[11] A. Abdulamit, D. Stematiu, and D. Gaftoi, " AN ALTERNATIVE METHOD TO EVALUATE THE HEALTH STATUS FOR CONCRETE DAMS.," *Environ. Eng. Manag. J.*, vol. 15, no. 6, pp. 1297–1407, Jun. 2016, Accessed: Jun. 17, 2021. [Online]. Available: tinyurl.com/3xxka2rf

[12] C. H. Loh, C. H. Chen, and T. Y. Hsu, "Application of advanced statistical methods for extracting long-term trends in static monitoring data from an arch dam," *Struct. Heal. Monit.*, vol. 10, no. 6, pp. 587–601, Nov. 2011, doi: 10.1177/1475921710395807.

[13] W. D. Zhao, "Statistical Analysis of Monitoring Data for Daniel Johnson Dam," McGill University Libraries, 2003. [Online]. Available: https://central.bac-lac.gc.ca/.item?id=TC-QMM-80156&op=pdf&app=Library

[14] Task Committee to Revise Guidelines for Dam, *Monitoring Dam Performance: Instrumentation and Measurements*. American Society of Civil Engineers, 2018. ISBN: 9780784414828

[15] G. Luzi, M. Crosetto, and O. Monserrat, "Advanced Techniques for Dam Monitoring," 2010. Accessed: Jun. 16, 2021. [Online]. Available: https://www.researchgate.net/publication/261180415

[16] L. Viman, S. Pop, and I. Ciascai, *Sisteme de achiziție de date: măsurarea traductoarelor cu coardă vibrantă și rezistive din construcțiile hidrotehnice*. Cluj-Napoca: Mediamira, 2015. ISBN: 978-973-713-322-8

[17] S. Pop, V. Bande, D. Pitica, and I. Ciascai, "Dynamic measurement circuit for the resistive

transducers,” in *2012 IEEE 18th International Symposium for Design and Technology of Electronics Packages, SIITME 2012 - Conference Proceedings*, 2012, pp. 259–262. doi: 10.1109/SIITME.2012.6384387.
[18] D. M. Ștefănescu, *Handbook of Force Transducers: Principles and Components*. Springer, 2011. ISBN: 978-3642182952
[19] A. I. Moisescu, “Evaluation of the safe operation of hydrotechnical construction, through acquisition system, transmission and processing significant parameters,” in *14th SGEM GeoConference on Water Resources. Forest, Marine and Ocean Ecosystems*, Jun. 2014, vol. 1. doi: 10.5593/sgem2014/b31/s12.035.
[20] A. Tavares, D. E. Castro, and M. J. Henriques, “Monitoring Planimetric Displacements in Concrete Dams,” May 2008.. [Online]: https://tinyurl.com/ffxb25jw
[21] V. Bande and S. S. Pop, “Triaxial Vibrating - Wire Transducer Implementation and Measurements,” in *SIITME 2019 - 2019 IEEE 25th International Symposium for Design and Technology in Electronic Packaging, Proceedings*, Oct. 2019, pp. 122–126. doi: 10.1109/SIITME47687.2019.8990716.
[22] J. Dunnicliff, *Geotechnical Instrumentation for Monitoring Field Performance | Wiley*. wiley, 1993. ISBN: 978-0-471-00546-9
[23] J. G. Webster and H. Eren, *Measurement, Instrumentation, and Sensors Handbook: Two-Volume Set*. CRC press, 2018. doi: https://doi.org/10.1201/9781315217109.
[24] G. Falkovich, *Fluid Mechanics*. Cambridge University Press, 2018. ISBN: 9781107129566
[25] C. S. Subramanian, H. Gurram, and P. L. Kanherkar, “A CFD and Experimental Study of Thin Flexible Wire in a Cross Flow,” 2016, p. 134.
[26] L. Viman, M. Dabacan, I. Ciascai, and S. Pop, “Embedded Microcontroller System for Reading Inductive Telependulum,” in *2007 30th International Spring Seminar on Electronics Technology (ISSE)*, May 2007, pp. 425–428. doi: 10.1109/ISSE.2007.4432893.
[27] “LEA_IT_PND4001001 Optical Coordinometer.” Accessed: May 03, 2020. [Online]. Available: https://tinyurl.com/6jrr4sr6
[28] A. Gil, L. A. Arguedas, and M. G. De Membrillera, “A proposal to optimize maintenance of dam monitoring systems,” 2012.
[29] I. Ciascai, L. Viman, and S. Pop, *Măsurarea electrică a traductoarelor din construcțiile hidrotehnice*. Casa cărții de știință, 2006. ISBN: 973-686-981-4
[30] American Society of Civil Engineers Task Committee on Instrumentation and Monitoring Dam Performance, *Guidelines for Instrumentation and Measurements for Monitoring Dam Performance*. ASCE, Reston, VA, 2000. ISBN: 0-7844-0531-X
[31] “LEA_IT_PND3101000 Electromagnetic Telependulum.” [Online]: https://tinyurl.com/yd6hjbcc
[32] “Telependul capacitiv tip WPS-2AP.” Accessed: May 06, 2020. [Online]. Available: http://www.automation.ro/pdf/fisa_prez_telependul_fogale.pdf
[33] I. Ciascai, *Senzori*, 1st ed. Cluj-Napoca: U.T.PRESS, 2018. ISBN: 978-606-737-335-6
[34] “Telependul tip TP 101-S.” Accessed: May 06, 2020. [Online]. Available: http://www.automation.ro/pdf/fisa_prez_TP101_S.pdf
[35] “Sistem optoelectronic de masurare a deplasarii barajelor-telependul optic model TP202.” Accessed: May 06, 2020. [Online]. Available: http://www.automation.ro/pdf/fisa_prez_pendulCCD.pdf
[36] Huggenberger, “TELELOT VDD2/3,” datasheet V4, Feb. 2019. [Online]: https://tinyurl.com/nrsjddx7
[37] I. Ciascai, *Sisteme electronice dedicate cu microcontrolere AVR RISC*. Cluj-Napoca: Editura Casa Cărţii de Ştiinţă, 2002. ISBN: 973-686-237-2
[38] F. Tavernier and M. Steyaert, *High-Speed Optical Receivers with Integrated Photodiode in Nanoscale CMOS*. Springer New York, 2011. ISBN: 9781441999252

[39] S. Pop, I. Ciascai, and D. Pitica, “Statistical analysis of experimental data obtained from the optical pendulum,” in *2010 IEEE 16th International Symposium for Design and Technology of Electronics Packages, SIITME 2010*, Sep. 2010, pp. 207–210. doi: 10.1109/SIITME.2010.5653515.
[40] J. Peatross and W. Michael, *Physics of Light and Optics*, 2015th ed. Lulu, 2015. ISBN: 9781312929272
[41] WorldSemi, “Inteligent control LED integrated light source,” WS2812B datasheet V5, Mar. 2019. Accessed: May 09, 2020. [Online]. Available: http://www.world-semi.com/DownLoadFile/108
[42] L. E. Frenzel, *Handbook of Serial Communications Interfaces: A Comprehensive Compendium of Serial Digital Input/Output (I/O) Standards*. Elsevier Science, 2015. ISBN: 9780128006719
[43] L. De Grandis, *Theory and Use of Color*. Abrams, 1986. ISBN: 9780810923171
[44] TAOS, “1536 × 1 Linear Sensor Array With Hold,” TSL1412S datasheet TAOS045F, Apr. 2007. Accessed: Jul. 18, 2018. [Online]. Available: https://pdf1.alldatasheet.com/datasheet-pdf/view/203049/TAOS/TSL1412S.html
[45] I. Ciascai and L. Ciascai, “Acquire images with a sensor and a microcontroller,” *EDN*, no. EDN | SEPTEMBER 23, 2010, p. 48, 2010.
[46] J. R. (John R. Taylor, *An introduction to error analysis : the study of uncertainties in physical measurements*. University Science Books, 1997. ISBN: 093570275X
[47] L. Wasserman, *All of Statistics: A Concise Course in Statistical Inference*. Springer New York, 2013. ISBN: 9780387217369
[48] D. G. Zill and M. R. Cullen, *Advanced Engineering Mathematics:*, no. v. 1. Jones and Bartlett Publishers, 2006. ISBN: 9780763745912
[49] S. M. Ross, *Introduction to Probability and Statistics for Engineers and Scientists.* Elsevier Science, 2009. ISBN: 9780080919379
[50] A. Mocan and I. Ciascai, “Analysis of positioning errors for LED,” in *2019 IEEE 25th International Symposium for Design and Technology in Electronic Packaging (SIITME)*, Oct. 2019, pp. 127–130. doi: 10.1109/SIITME47687.2019.8990720.
[51] M. N. Khan, *Understanding LED Illumination*. CRC Press, 2013. ISBN: 9781466507739
[52] R. Khandpur, *Printed Circuit Boards : Design, Fabrication, and Assembly: Design, Fabrication, and Assembly*. Mcgraw-hill, 2005. ISBN: 9780071464208
[53] P. D. Rufe, *Fundamentals of Manufacturing, Second Edition*. Society of Manufacturing Engineers, 2002. ISBN: 9780872635241
[54] L. J. Zheng *et al.*, “Experimental Study of Micro-holes Position Accuracy on Drilling Flexible Printed Circuit Board,” in *Global Conference on Sustainable Manufacturing*, 2013, pp. 268–272. ISBN: 9783798326095
[55] Foryard Optoelectronics, “FYL-5013PURD1C PRODUCT SPECIFICATION,” datasheet A. [Online]. Available: http://www.foryard.com/x-en/p-download/d-Part/u-f/m-1/n-f_FYL-5013PURD1C/y-179
[56] “IPC-2222 Sectional Design Standard for Rigid Organic Printed Boards,” 1998. Accessed: Aug. 03, 2019. [Online]. Available: http://www.ipc.org/toc/ipc-2222.pdf
[57] R. STRAUSS, *SMT Soldering Handbook*. Elsevier Science, 1998. ISBN: 9780080480978
[58] C. T. Robertson, *Printed Circuit Board Designer’s Reference: Basics*. Prentice Hall Professional Technical Reference, 2004. ISBN: 9780130674814
[59] A. E. Schwaneke, W. L. Falke, and U. S. B. of Mines, *Surface Tension and Density of Liquid Tin*. U.S. Department of Interior, Bureau of Mines, 1970. [Online]. Available: https://books.google.ro/books?id=KgGoD682BQgC
[60] R. Prasad, *Surface Mount Technology: Principles and Practice*. Springer US, 2013. ISBN: 9781461540847

[61] T. L. Landers, *Electronics Manufacturing Processes*. Prentice Hall, 1994. ISBN: 9780131764705
[62] S. Pop, I. Ciascai, V. Bande, and D. Pitica, “Modeling the light of LED’s for position detection with an optical sensor,” in *33rd International Spring Seminar on Electronics Technology, ISSE 2010*, May 2010, pp. 374–377. doi: 10.1109/ISSE.2010.5547321.
[63] B. D. Guenther, *Modern optics*. Wiley, 1990. ISBN: 0471605387
[64] J. P. Dakin and R. Brown, *Handbook of Optoelectronics: Concepts, Devices, and Techniques (Volume One)*. CRC Press, 2017. ISBN: 9781482241792
[65] B. Crowell, *Optics*. Light and Matter, 2003. ISBN: 0970467052
[66] R. Larson, R. P. Hostetler, and B. H. Edwards, *Trigonometry: A Graphing Approach*. D.C. Heath, 1995. ISBN: 9780669282962
[67] B. Riegler and R. Thomaier, “Index matching silicone for optoelectronic applications,” in *New Developments in Optomechanics*, Sep. 2007, vol. 6665, p. 666508. doi: 10.1117/12.735950.
[68] I. Ciascai and A. Mocan, “Calibration procedure for pendulum position measurement,” *Acta Tech. Napocensis - Ser. Appl. Math. Mech. Eng.*, vol. 63, no. 1, pp. 21–26, 2020, [Online]. Available: https://atna-mam.utcluj.ro/index.php/Acta/article/view/1286
[69] D. Kirk and O. for Higher Education (Firm), *Graphics Gems III (IBM Version)*. Morgan Kaufmann, 2012. ISBN: 978-0-12-409673-8
[70] A. Mocan and I. Ciascai, “A model for measuring the position of a pendulum using opto-electronic method,” *Acta Tech. Napocensis - Ser. Appl. Math. Mech. Eng.*, vol. 61, no. 4, pp. 603–608, Dec. 2018, Accessed: Feb. 16, 2019. [Online]. Available: https://atna-mam.utcluj.ro/index.php/Acta/article/view/1101
[71] Jon Skeet, *C# in Depth*, 3rd ed. 2017. ISBN: 9781548844738
[72] J. Greene and A. Stellman, *Head First C#: A Learner’s Guide to Real-World Programming with C#, XAML, and. NET*. “ O’Reilly Media, Inc.,” 2013. ISBN: 9781449358884
[73] H. Buckley, *WPF for IT Students*. CreateSpace Independent Publishing Platform, 2016. ISBN: 9781533040282
[74] C. Sells and I. Griffiths, *Programming Windows presentation foundation*, 2nd ed. “ O’Reilly Media, Inc.,” 2007. ISBN: 978-0-596-51037-4
[75] A. Thorn, *DirectX 9 User Interfaces: Design and Implementation*. Wordware Pub., 2004. ISBN: 9781556222498
[76] C. Sells, *Windows Forms Programming in C#*. Addison-Wesley, 2004. ISBN: 9780321116208
[77] F. Yuan, *Windows Graphics Programming: Win32 GDI and DirectDraw*. Prentice Hall PTR, 2001. ISBN: 9780130869852
[78] M. J. Price, *C# 8.0 and .Net Core 3.0*, 4th ed. Packt Publishing, 2019. ISBN: 978-1788478120
[79] S. Gamse, M. J. Henriques, and M. Oberguggenberger, “Assessment of long term pendulum and geodetic observations on a concrete arch dam,” in *3rd Joint International Symposium on Deformation Monitoring*, 2016, pp. 1–8. Accessed: May 14, 2021. [Online]. Available: https://tinyurl.com/ep22h89s
[80] A. Mocan, I. Ciascai, and A. Ciascai, “Simulations of Measurement Errors for a Pendulum Reader,” May 2021. doi: https://doi.org/10.1109/ISSE51996.2021.9467634.
[81] STMicroelectronics, “Medium-density performance line ARM-based 32-bit MCU with 64 or 128 KB Flash, USB, CAN, 7 timers, 2 ADCs, 9 communication interfaces,” STM32F103x8, STM32F103xB datasheet 13587; Rev 17, Aug. 2015. Accessed: Jun. 12, 2020. [Online]. Available: https://www.st.com/resource/en/datasheet/stm32f103c8.pdf
[82] D. Norris, *Programming with STM32 : getting started with the Nucleo Board and C/C++*. 2018. ISBN: 9781260031317 1260031314

[83] “Software development tools STM32 and STM8 microcontrollers,” Jan. 2021. Accessed: Jun. 23, 2021. [Online]. Available: https://tinyurl.com/3ykcyv4z
[84] B. W. Kernighan, *C Programming Language (2E)*. Prentice Hall, 2005. ISBN: 9780131193710
[85] B. Stroustrup, *The C++ Programming Language*. Addison-Wesley, 2000. ISBN: 9780201700732
[86] S. Klabnik and C. Nichols, *The Rust Programming Language*. No Starch Press, 2019. ISBN: 9781718500457
[87] K. Nacke, *Learn LLVM 12: A beginner’s guide to learning LLVM compiler tools and core libraries with C++*. Packt Publishing, 2021. ISBN: 9781839210037
[88] W. von Hagen, *The Definitive Guide to GCC*. Apress, 2011. ISBN: 9781430202196
[89] R. Clark, “Arduino STM32 NeoPixels (WS2812B) using SPI DMA,” 2017. https://www.rogerclark.net/arduino-stm32-neopixels-ws2812b-using-spi-dma/ (accessed Jun. 13, 2020).
[90] W. Gay, *Beginning STM32*. Apress, 2018. doi: https://doi.org/10.1007/978-1-4842-3624-6.
[91] E. White, *Making Embedded Systems: Design Patterns for Great Software*. 2011. ISBN: 9781449320584
[92] R. Oshana, Ed., *DSP for Embedded and Real-Time Systems*. Newnes, 2012. doi: 10.1016/C2010-0-67143-4.
[93] P. Acarnley, *Stepping Motors: A Guide to Theory and Practice*. Institution of Engineering and Technology, 2002. ISBN: 9780852964170
[94] D. S. Nyce, *Position Sensors*. Wiley, 2016. ISBN: 9781119069355
[95] I. Griffiths, *Programming C# 8.0: build cloud, web, and desktop applications*. O’Reilly Media, Inc., 2020. ISBN: 978-1492056812
[96] “Asynchronous programming in C# | Microsoft Docs.” https://docs.microsoft.com/en-us/dotnet/csharp/programming-guide/concepts/async/ (accessed Jul. 07, 2020).
[97] J. E. Gentle, *Random Number Generation and Monte Carlo Methods*, 2nd ed. Springer, 2005. ISBN: 0387001786
[98] D. Pilone and N. Pitman, *UML 2.0 in a Nutshell*. O’Reilly, 2005. ISBN: 9780596007959
[99] R. S. Polimeni, F. J. Fabozzi, A. H. Adelberg, and J. A. Burke, *Product Costing: Concepts and Applications*. McGraw-Hill Higher Education, 1999. ISBN: 9780072390841
[100] G. K. Mislick and D. A. Nussbaum, *Cost Estimation: Methods and Tools*. Wiley, 2015. ISBN: 9781118536131
[101] “Coordiscop pentru masurare penduli-2 bucati,” 2015. https://www.licitatie-publica.ro/licitatii/coordiscop-pentru-masurare-penduli-2-bucati?uuid=49f2769a-7461-11e5-aee8-002655ffd6c8 (accessed Jun. 26, 2021).
[102] “DWL9000XY 2-Axis Ultra Precision Inclinometer,” User manual, 2021. Accessed: Jun. 06, 2021. [Online]. Available: www.digipas.com
[103] P. J. Hoffman, *Precision Machining Technology*. Delmar Cengage Learning, 2012. ISBN: 9781111308063
[104] G. Strang, *Introduction to Linear Algebra*. Wellesley-Cambridge Press, 1993. ISBN: 9780961408824
[105] D. Hestenes, *New Foundations for Classical Mechanics*. Dordrecht: Kluwer Academic Publishers, 1999. ISBN: 0-7923-5514-8
[106] I. Prasojo, A. Maseleno, O. tanane, and N. Shahu, “The Design of Earthquake Detector Using Pendulum Swing Based on ATMega328,” *J. Robot. Control*, vol. 2, no. 3, pp. 209–211, May 2021, doi: 10.18196/jrc.2380.
[107] D. Regalado et al., Gray Hat Hacking The Ethical Hacker’s Handbook, 5th ed. McGraw-Hill, 2018. ISBN: 9781260108422